

Response of Glass Fiber Reinforced Polymer (GFRP)-Steel Hybrid Reinforcing Bar in Uniaxial Tension

Minkwan Ju¹⁾, Sangyun Lee²⁾, and Cheolwoo Park³⁾*

(Received July 4, 2016, Accepted July 9, 2017, Published online December 7, 2017)

Abstract: This study introduces a glass fiber reinforced polymer (GFRP)-steel hybrid bar with a core of a deformed steel bar (steel core). Six types of the hybrid cross section were considered, and a total of 48 tensile specimens were tested by the uniaxial tensile test to measure the tensile strength and modulus of elasticity of the GFRP hybrid bar. The results of the uniaxial tensile test revealed that the GFRP hybrid bar showed higher modulus of elasticity and lesser ultimate tensile strength than those shown by a normal GFRP bar. The stress–strain relationship showed a bi-linear behavior indicating good ductility against the brittle failure of a normal GFRP bar. Among all the steel core having a diameter of 19.1 mm, the bar with a core diameter of 9.53 mm exhibited the highest tangent modulus of elasticity. A tensile stress–strain model was suggested for the GFRP hybrid bar having an outer diameter of 19.1 mm and a core diameter of 9.53 mm. This was in good agreement with the experimental results. The suggested stress–strain model can be applied for structural design or analysis of concrete structures such as bridge deck slabs.

Keywords: GFRP- and deformed steel hybrid bars, modulus of elasticity, durability, uniaxial tensile test, stress–strain model.

1. Introduction

Structural degradation of reinforced concretes (RCs) occurs mainly because of the corrosion of steel reinforcements due to the penetration of de-icing salts on RC bridge deck slabs or carbonation of concrete by environmental attacks during the service life. To prolong the service life of reinforced concrete, some research to prevent corrosion of reinforcing steel have been performed. Pritzl et al. (2014) found out that the acrylic coating was effective to prevent corrosion of steel bar. Choi et al. (2008, 2006) reported that epoxy-coated steel bar showed good performance under corrosive environment. Tae (2006) proved that the Cr-bearing rebar with over 7% of Cr content possessed excellent corrosion resistance.

Another innovative approach to prevent reinforcement from the corrosion is to use a glass fiber reinforced polymer (GFRP)

bar as a reinforcement in reinforce concrete. Owing to their non-corrosiveness and high tensile strength, glass fiber reinforced polymer (GFRP) bars are considered as promising alternatives to RCs (Maranan et al. 2015; El-Gamal et al. 2009). Another advantage of GFRP bars is their low cost as compared to that of the fiber reinforced polymers (FRPs) made up of carbon or aramid (Zheng et al. 2012; Carvelli et al. 2010; El-Gamal et al. 2007). However, GFRP bars suffer from service-related issues which still need to be addressed such as large deflection or crack width in structural design because of the high deformability caused by the low modulus of elasticity (Mazaheripour et al. 2016). Several efforts have been made for enhancing the flexural stiffness of GFRP bar reinforced concretes by using the GFRP and steel reinforcements simultaneously (El-Refai et al. 2015; Lau and Pam 2010). It was found that these GFRP bar reinforced concretes showed an improved flexural capacity with less crack width and lower deflection in the serviceability. This approach may have a limitation due to a complicated arrangement of reinforcements during the construction and the lack of design specification because of the composite action between the GFRP and the steel bars. Several studies have been conducted with an aim to improve the flexural stiffness of FRP bars using hybrid rods. Nanni et al. (1994) developed a hybrid rod consisting of FRP braided skin made up of aramid or vinylon fiber and a steel core. It was found that the hybrid rod had a modulus of elasticity higher than that of the normal FRP bar and exhibited a bi-linear behavior in ductile manner. A hybridization approach was studied by You et al. (2007). They observed that the hybrid FRP bar with a core of carbon fiber showed an improvement in the modulus of elasticity. It was found that the modulus of elasticity of this hybrid bar was higher than that of glass fibers. On the basis of these studies, it can be

¹⁾Department of Civil and Environmental Engineering, Yonsei University, 50 Seodaemun-gu, Seoul 03722, Republic of Korea.

²⁾Korea Institute of Civil Engineering and Building Technology, 315 Goyang-dae-ro, Ilsan-seo-gu, Goyang-Si, Gyenggi-Do 10223, Republic of Korea.

³⁾Department of Civil Engineering, Kangwon National University, 346 Joongang-ro, Samcheok-si, Kangwon 25913, Republic of Korea.

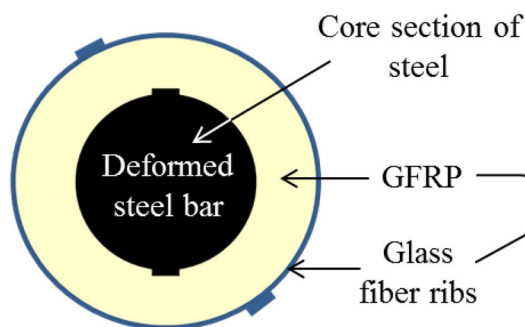
*Corresponding Author; E-mail: tigerpark@kangwon.ac.kr

stated that FRP-hybrid steel bars can be promising alternative reinforcements to normal GFRP bars. Seo et al. (2013) investigated the tensile characteristics of the GFRP hybrid bars with a GFRP outer surface having a diameter of 12.7 mm and a deformed steel core having a diameter of 9.0 mm. It was revealed that the hybridization could improve the modulus of elasticity and enabled the enhancement of the flexural stiffness of reinforced concretes. In this study, the GFRP hybrid bar with unique properties such as non-corrosiveness and high modulus of elasticity was produced. The GFRP hybrid bars can provide structural efficiency to the RCs having low crack width and deflection as compared to normal GFRP bars and exhibit better serviceability in flexure. The GFRP hybrid bars also contribute to the durability of concretes because of the non-corrosiveness of the GFRP surface. Moreover, GFRPs are relatively cost effective as compared to carbon or aramid fibers. With regard to the structural design, several guidelines have been proposed for designing the reinforced concretes using GFRP bars (ACI 440.1R-15 2015; AASHTO 2009; CSA S806-12 2012). The material and mechanical characteristics of the GFRP hybrid bars can be studied and reflected in those structural designs.

The current study aims to investigate the tensile property of the GFRP hybrid bars experimentally. A total of 48 tensile specimens were tested by the uniaxial tensile test in accordance with the ASTM test method (ASTM D 3916 2002). The test specimens had geometrical variables in a cross section consisting of an outer GFRP surface and a deformed steel bar (steel core). In order to compare the enhanced tensile strength of the GFRP hybrid bars with the steel core, the tensile test was conducted for the steel core of D10, D13, and D16, respectively. The important and fundamental mechanical properties including tensile strength, stress-strain relationship, and modulus of elasticity were investigated. In addition, a stress-strain model for the GFRP hybrid bar was suggested. The application of hybrid bar as a tensile reinforcement in structural designs was also discussed.

2. Description of GFRP and Deformed Steel Hybrid Bar

Figure 1 shows the geometry and complete product of the GFRP hybrid bar. The cross section comprised of three parts:



the core section of the deformed steel bar, outer surface of the GFRP, and braided fiber ribs on the surface. These configurations help in achieving a perfect composite action. Besides, bond between steel bar and GFRP outer surface is guaranteed due to strong friction property by steel ribs after the thermosetting processing. The GFRP hybrid bar was manufactured by a typical pultrusion-thermosetting process shown in Fig. 2 (Park et al. 2016). Glass fiber strands bound with a thermosetting vinyl ester resin were formed at the outer surface of the core of the deformed steel bar. The modulus of elasticity was significantly enhanced by the steel core and was more than that of a normal GFRP bar. Moreover, the braided fiber ribs strengthened the bonding of the GFRP hybrid bar with the surrounding concrete, thus enhancing the mechanical interlocking. This uneven surface treatment could improve the shear resistance of the concrete reinforced with the GFRP hybrid bar against the pulling of the GFRP hybrid bar under a uniaxial or flexural behavior.

3. Experimental Program

3.1 Test Specimens

The material properties of E-glass fibers and vinyl ester resins were investigated in a previous study (You et al. 2015). The fiber volume content of the normal GFRP bars was found to be 78.0%. For the fiber ribs, a commercial Kuralon filament provided by Kuraray Company was used. The deformed steel core had a yield strength of 400 MPa. Table 1 lists the test variables of the GFRP hybrid bar. A total of eight types of variables and 48 specimens were tested under the uniaxial tensile scheme. The nominal diameter of the GFRP hybrid bar was within the range of 12.7–19.1 mm. The core had a diameter lying in the range of 9.53–15.9 mm. The normal GFRP bar with a diameter of 15.9 mm was not available for comparison due to the lack of material quality. The outer diameter was used as the nominal diameter to calculate the tensile strength of the GFRP hybrid bar. The pitch space of the fiber ribs was designed to be equal to the nominal diameter of the GFRP hybrid bar.

Figure 3 shows the tensile test specimens of the GFRP hybrid bar. In contrast to the steel bar, the bar with a GFRP surface needed an additional mechanical anchorage



Fig. 1 Geometry and product of GFRP and deformed steel hybrid bar.

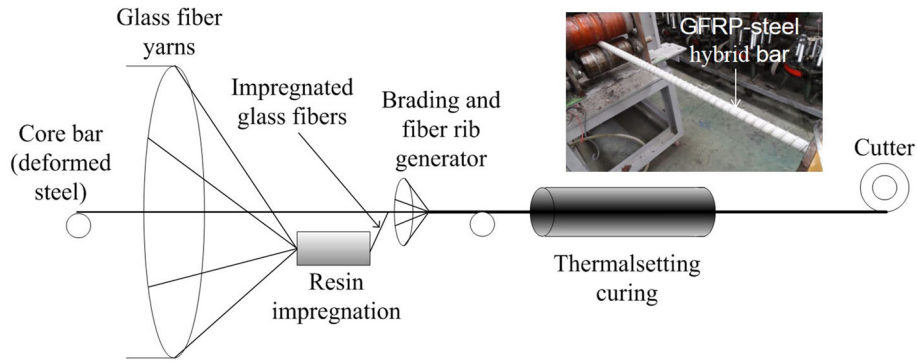


Fig. 2 Pultrusion and thermosetting process of sand coated GFRP and deformed steel hybrid bar.

Table 1 Details of the GFRP hybrid bar.

Specimen no.	Specimen ID	Nominal diameter (core diameter) (mm)	Pitch space of fiber ribs (mm)	Number of samples
1	D13	12.7	12.8	6
2	D13 (D10)	12.7 (9.53)	12.8	6
3	D16 (D10)	15.9 (9.53)	15.9	6
4	D16 (D13)	15.9 (12.7)	15.9	6
5	D19	19.1	19.1	6
6	D19 (D10)	19.1 (9.53)	19.1	6
7	D19 (D13)	19.1 (12.7)	19.1	6
8	D19 (D16)	19.1 (16.1)	19.1	6

depending on the diameter of the GFRP hybrid bar in compliance with ACI 440 3R-04 (2004). The specification recommends a gripping metal tube in the connecting grips of

the testing machine. Using a steel tube with filled mortar, the surface damage caused by the transverse compressive strength acting on the GFRP hybrid bar can be avoided. In

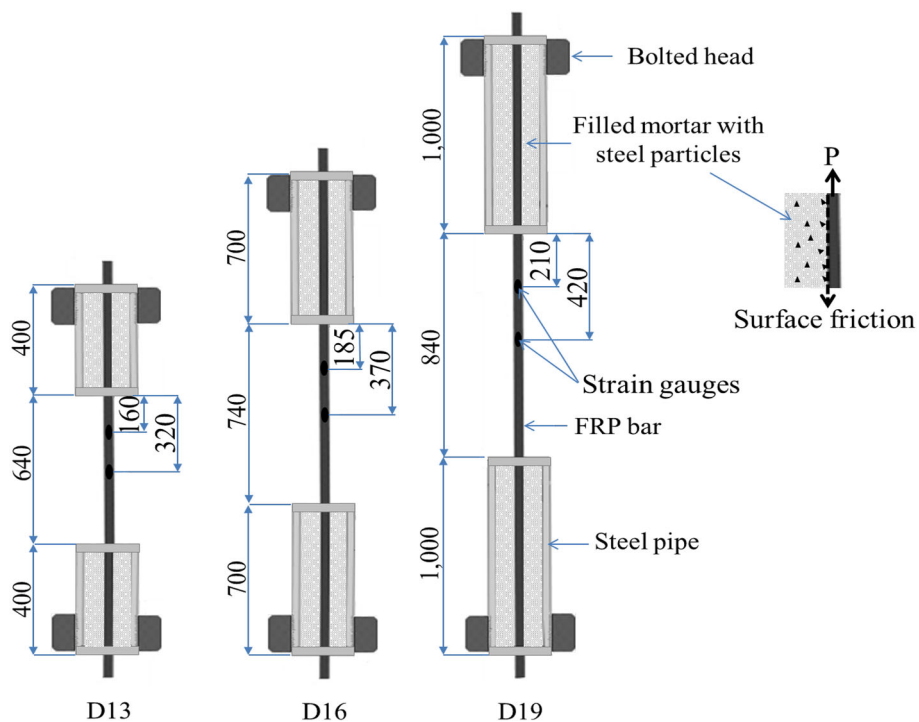


Fig. 3 Details of test specimens (unit in mm).

this study, however, both the ends of the metal tube were equipped with headed bolts, and the tensile load was directly applied at the headed bolts along the longitudinal direction without any transverse compressive strength. This gripping detail could reduce the metal anchorage length against the friction grip type. In order to enhance the friction between the filled mortar and the GFRP hybrid bar, steel particles were additionally mixed into the mortar. The mixing ratio was 14% for mortar and 86% for water, and the mixture was cured under laboratory conditions for 14 days. The compressive strength of the mortar was found to be 67.5 MPa.

3.2 Test Setup and Strain Measurement

The GFRP hybrid bar was fixed to the upper grip of a universal test machine (UTM) with a load of 1000 kN. The test was carried out automatically under a displacement control with a loading rate of 5 mm/min for the D13 and D16 specimens, while the D19 specimen had a loading rate of 2 mm/min considering the lesser volume of filled mortar in it. Strain gauges were installed at the $L/2$ and $L/4$ of the FRP bar to investigate the strain variation in the longitudinal direction. Figure 4 shows the schematic of the test setup.

4. Results and Discussions

4.1 Load-Slip Relationship

The slip between the GFRP hybrid bar and filled mortar in the anchorage tube is vulnerable because of the test configuration. Therefore, before investigating the stress–strain relationship, the slips at both the loadings and fixed ends were carefully investigated. If a slip occurs beyond an allowable level, the tensile stress may not be accurate because of the lost tensile force contributed to the slip behavior. The difference between the length at the loading end (δ_u) and that at the fixed end (δ_d) was measured and compared before and after the tensile test. Figure 5 shows

the measured average slip at each end. By averaging the change in the length and taking it as the absolute value, the maximum slip in the normal D13 and D19(D10) bars was found to be 4.0% (0.512 mm) and 2.6% (0.5 mm) for the pitch space of 12.8 and 19.1 mm, respectively. These values may be small enough not to affect the stress–strain relationship.

4.2 Tensile Stress–Strain Relationship

The measured stress–strain relationship of the GFRP hybrid bars for the representative test specimens are shown in Fig. 6. By comparing the strain values at $L/2$ and $L/4$, the even distribution of stress throughout the free length of the GFRP hybrid bar was confirmed. The values were almost identical so that it was known that the applied stress was evenly distributed along the longitudinal direction. For the D16 bar shown in Fig. 6b, the tensile stress–strain of the normal D13 GFRP bar was additionally imposed to indirect comparison with that of the D16 bar. Due to the hybridization of a steel core and a GFRP outer surface, the tensile stress–strain behavior was governed by a bi-linear manner. The modulus of elasticity for the GFRP hybrid bar and normal GFRP bar were compared. As a result, the hybrid bar showed an apparent increase in the modulus of elasticity by the yielding point of the steel core. This phenomenon was observed for all the hybrid bar specimens. It was found that the initial modulus of elasticity of the GFRP hybrid bar was governed by the core of the deformed steel bar. Hence, the present design of steel reinforced concrete was valid up to the initial modulus of elasticity. This state could determine the serviceability of the crack width and deflection. However, the tangent modulus of elasticity in the first linear branch exhibited much less stiffness as compared to that in the second linear branch. In order to compare the enhanced tensile strength of the GFRP hybrid bars with the steel core, the tensile test was conducted for the steel core of D10, D13, and D16, respectively. The yield strength was 400 MPa and

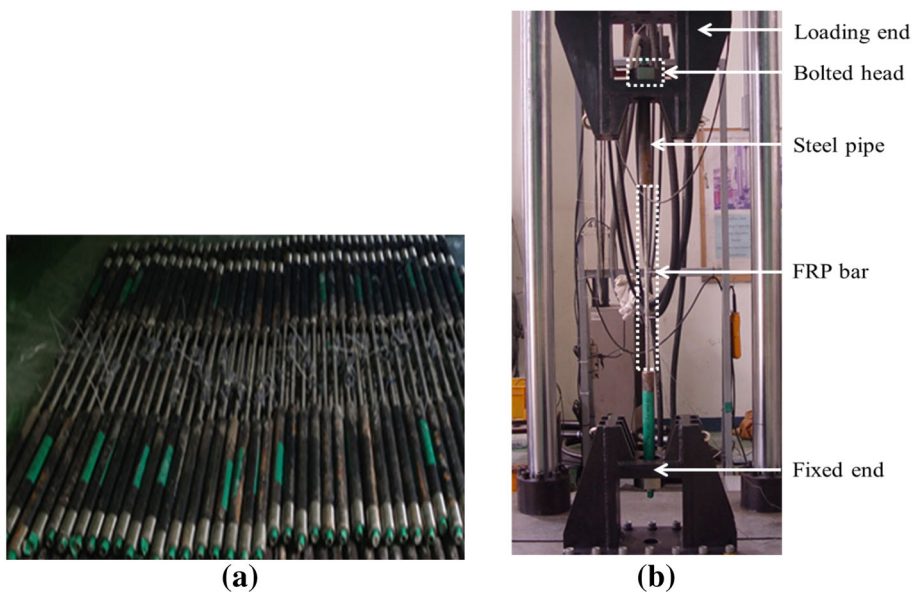


Fig. 4 Test specimens and set up. a Fabricated test specimens, b Test set up

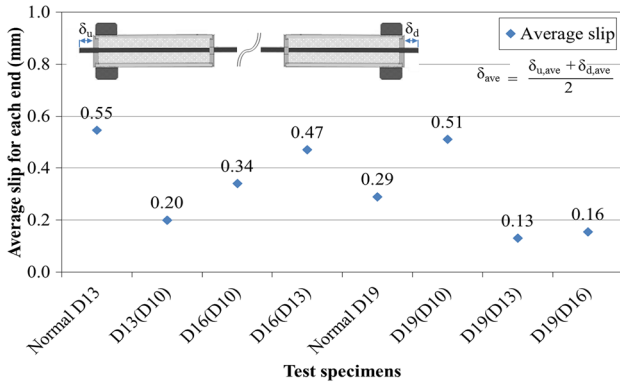
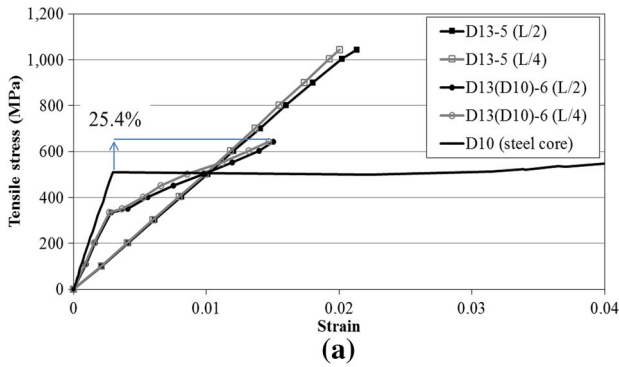
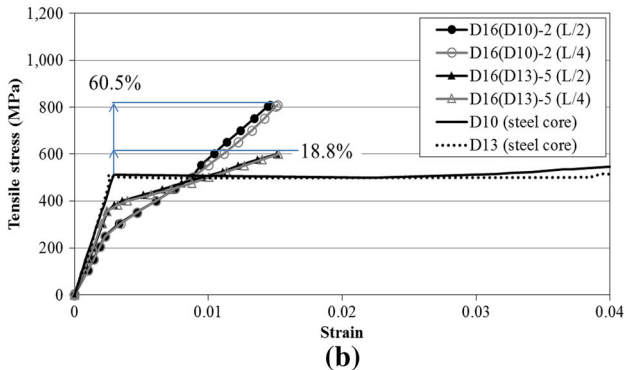


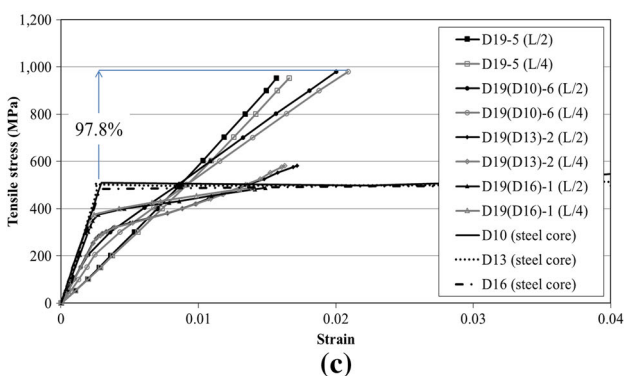
Fig. 5 Average slip measurement at both ends.



(a)



(b)



(c)

Fig. 6 Tensile stress–strain relationships of the GFRP hybrid bars. a D13 specimen series, b D16 specimen series, c D19 specimen series

the number of specimens was three for each diameter. Only one of the tensile stress data for each diameter was plotted in Fig. 6 because the tensile stress–strain behaviors of steel core were identical. It was found that the increased ranges of tensile strength showed from 18.8 to 97.8% as compared

to the yield strength of steel core. As the amount of GFRP outer surface increased, the enhanced effect of tensile strength was increased too. Among the GFRP hybrid bars, D19(D10) specimen showed the largest increase of tensile strength. It was judged that the hybridization of the GFRP and steel core can devote to the higher tensile strength than the steel core and the higher modulus of elasticity than the normal GFRP bar.

The result of the second branch was strongly dependent on the sectional area of the GFRP outer surface. From Fig. 6c, it can be observed that the tangent modulus of elasticity increased with an increase in the sectional area of the GFRP outer surface. However, the modulus of elasticity decreased as a result of the increase in the tangent modulus of elasticity. The average tensile strength of six specimens was measured for each test variable and is summarized in Table 2. The average tensile strengths of the normal D13 and D19 GFRP bars were found to be 1120.2 and 903.4 MPa, respectively. It was found that the average tensile strength of the GFRP hybrid bar was much less than that of the normal GFRP bar, and the magnitude was influenced by the area of the GFRP outer surface. The ultimate tensile strength was determined by the amount of GFRP at the outer surface. For the configuration of the all same core section of D10 deformed steel bar, the GFRP hybrid bar with a D19 GFRP outer surface showed a tensile strength higher than that of the GFRP hybrid bar with a D13 GFRP outer surface. It was revealed that the tensile property of the GFRP hybrid bar was mainly governed by how the area ratio between the steel core and the GFRP outer surface was configured. Moreover, Fig. 6 confirmed that GFRP could lead to strain hardening once the steel core reached the yield strain. This can be explained by the fact that both the GFRP hybrid bar underwent a good composite action under the uniaxial tensile behavior.

Figure 7 shows the tensile stress–strain relationship of the GFRP hybrid bar when only the area of the GFRP outer surface was varied. The results suggested that the magnitude of the ultimate strength was proportionally governed by the amount of GFRP in the outer surface. As compared to the other specimens the D13(D10) specimen exhibited less strain hardening after the yielding of the steel core. This could be attributed to the fact that the area of the GFRP outer surface was relatively small and the stress–strain relationship was slightly governed by the plastic behavior of the steel core at the E_T branch. As the area of the GFRP increased, the modulus of elasticity at the first branch was decreased and the tangent modulus of elasticity was increased. The optimum relationship between the tensile strength and the modulus of elasticity for structural designs needs to be investigated and discussed.

4.3 Investigation of Tensile Strength, Modulus of Elasticity and Cross Sectional Ratio

Figure 8 shows the relationship between the tensile strength and the modulus of elasticity of the GFRP hybrid bar. The modulus of elasticity was calculated according to CSA S806-12. The equation consisted of the applied loads

Table 2 Tested tensile strength of the GFRP hybrid bar.

	D13	D13 (D10)	D16 (D10)	D16 (D13)	D19	D19 (D10)	D19 (D13)	D19 (D16)
1	1108.5	649.7	768.3	591.5	957.0	893.1	561.2	483.0
2	1125.1	704.0	818.8	611.0	872.6	910.2	576.0	498.4
3	1112.8	680.0	794.3	613.1	924.7	845.2	534.7	438.4
4	1174.9	–	805.6	611.6	858.2	854.6	535.3	490.9
5	1091.6	–	799.9	606.2	942.2	922.1	413.5	473.6
6	1108.5	–	805.8	634.1	865.7	970.0	536.7	472.7
Average tensile strength (MPa)	1120.2	677.9	798.8	611.3	903.4	899.2	526.2	476.2
Standard deviation (MPa)	24.4	22.2	15.5	12.5	39.3	42.0	52.7	19.2

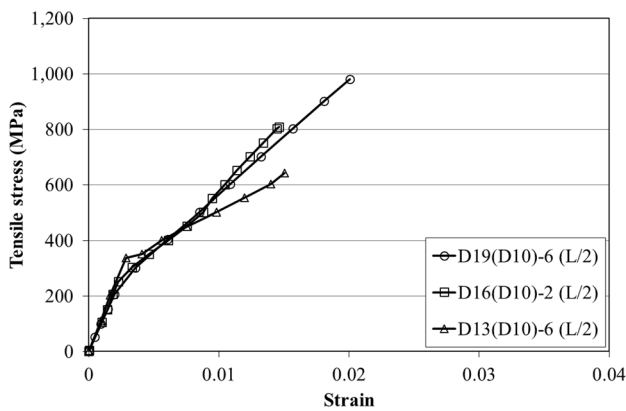


Fig. 7 Tensile stress–strain relationship according to the area of GFRP outer surface.

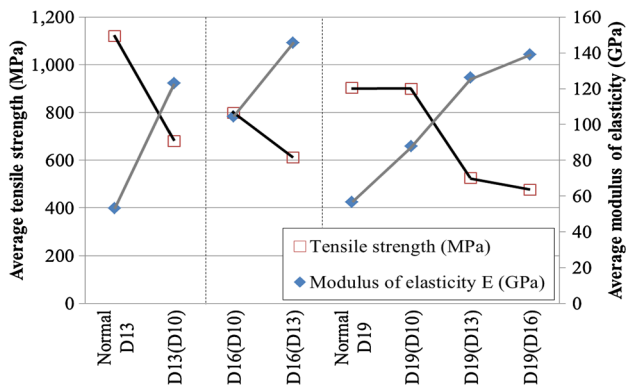


Fig. 8 Relationship between tensile strength and modulus of elasticity.

P_1 and P_2 corresponding to 50 and 25% of the ultimate load, respectively, and the corresponding strains ϵ_1 and ϵ_2 . This equation showed an inverse relationship. Thus, if the area of GFRP outer surface was increased, an increase in the tensile strength was observed, while the magnitude of the modulus of elasticity decreased. This relationship is quite important to determine the design parameters of the GFRP hybrid bar as a longitudinal reinforcement. An optimum balance between

the tensile strength and the modulus of elasticity should be established to obtain hybrid reinforcements with optimum tensile properties. Though the number of test variables used in this study was not sufficient, we aimed to solve the abovementioned issues using an approach illustrated in Fig. 8. The number of variables was limited by the compliance to the specified standard diameter of the reinforcement. A reasonable criteria for the sectional design was the intersection point between the positive and negative inclination curves for the tensile strength and modulus of elasticity for the D13, D16, and D19 specimens, respectively.

Keeping the difficulty in adjusting the sectional design according to the standard diameter in mind, the sectional design of the GFRP hybrid bar with a core of D10 steel core was considered to be the most appropriate design. The modulus of elasticity for this structural design was found to be 87.8 GPa, which was 154.9% of that of the normal D19 GFRP bar. Moreover, there were the least change of tensile strength within 0.5%.

Figure 9 is the results of investigation of yield stress and modulus of elasticity relationship. This analysis is important for guaranteeing the material property for each test specimens with varying cross sectional ratio, inner and outer diameter of the GFRP hybrid bars. It may be also directly associated with the manufacturing quality.

It must be very important aspect for design using the GFRP hybrid bar as the experimental data in tensile can be converged well. In the result of the analysis, D19(D10) hybrid bar showed the most accurate relationship for yield stress and modulus of elasticity, while D16(D10) and D19(D16) showed good results except some of out of data. This result proved that D19(D10) hybrid bar has the most stable behavior in tensile test.

Table 3 shows the calculated results for the modulus of elasticity (E) and tangent modulus of elasticity (E_T). The variation in E_T was found to be proportional to that in the area of the GFRP outer surface. Figure 9 shows the relationship between the tangent modulus of elasticity and the cross sectional ratio of the GFRP hybrid bar. After

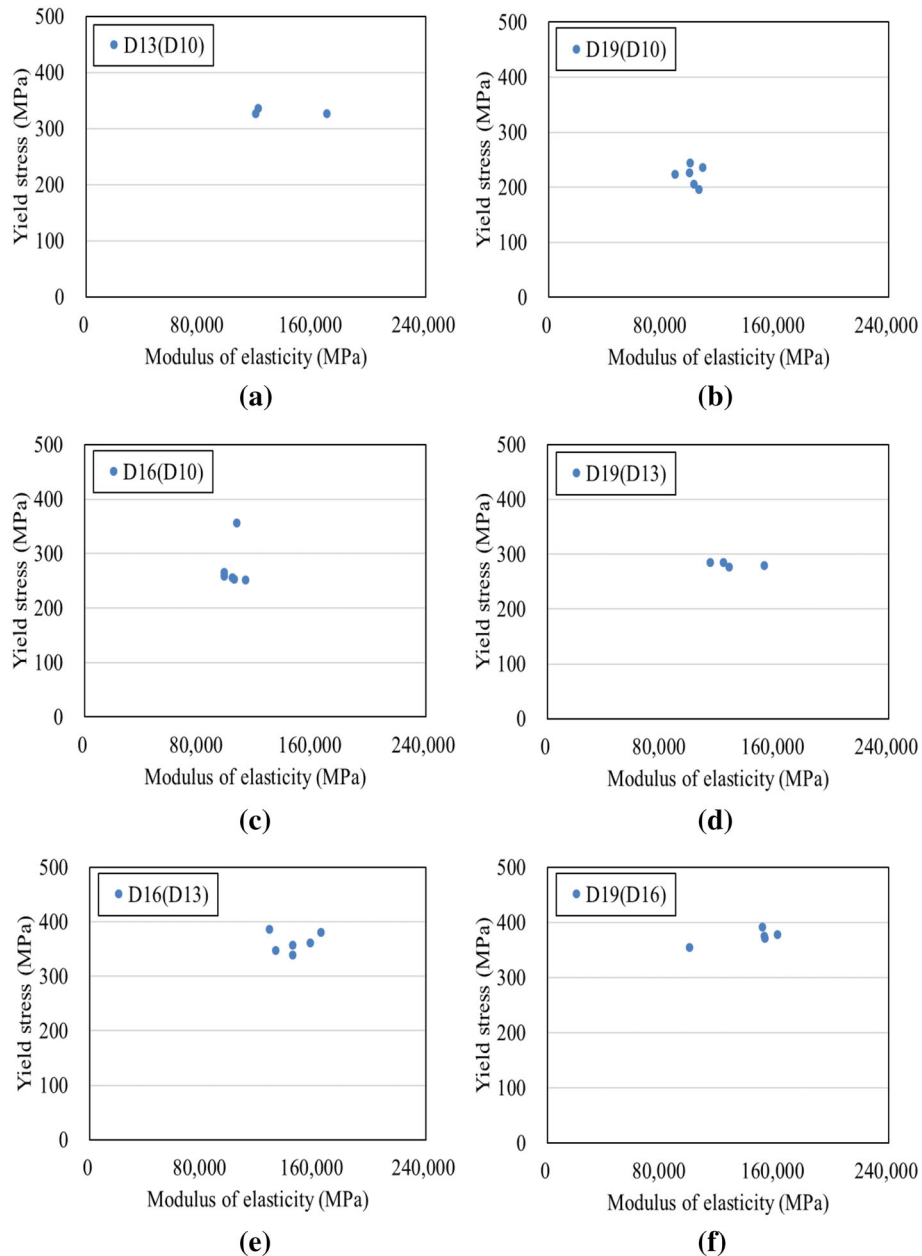


Fig. 9 Yield stress and modulus of elasticity relationship. **a** D13(D10) specimens, **b** D16(D10) specimens, **c** D16(D13) specimens, **d** D19(D10) specimens, **e** D19(D13) specimens, **f** D19(D16) specimens

approaching the yield strain of the steel core, the tensile behavior of the second branch is governed by the GFRP outer surface.

Thus, E is transferred to E_T because its behavior is governed by the low modulus of elasticity of the GFRP. The ultimate tensile properties such as the design tensile strength and the modulus of elasticity should be determined within the E_T branch. This is because the strain hardening property is still available for stress transfer to the concrete. Moreover, an interesting aspect was identified in Fig. 10. The E_T and cross sectional ratio showed a close correlation. Once the cross sectional ratio was determined, the E_T could be approximately estimated except for the D16 specimen series.

This large discrepancy might be due to incomplete material configuration.

From the analysis of the relationship between the tensile strength and the modulus of elasticity, including the tangent branch, it was found that the design of the D19(D10) hybrid bar was appropriate and displayed high E_T and low discrepancy in the cross sectional ratio. Therefore, it had an excellent tensile stiffness at the mechanical range of E and E_T branch along with a sufficiently high tensile strength. A material model of E_T with an appropriate safety factor may be analytically obtained according to the varying cross sectional ratios by attaining a quality control with an effective design process.

Table 3 Average modulus of elasticity and tangent modulus of elasticity.

	D13(D10)	D16(D10)	D16(D13)	D19(D10)	D19(D13)	D19(D16)
Average modulus of elasticity						
Average E (GPa)	123.0	104.4	145.5	87.8	126.2	139.1
Standard deviation (GPa)	12.7	3.8	12.7	4.4	10.2	26.5
Tangent modulus of elasticity						
1	25.0	52.3	18.5	40.1	22.5	10.9
2	22.2	34.0	57.1	42.8	16.9	10.6
3	23.0	65.0	14.1	41.9	37.1	5.2
4	15.7	57.1	19.9	40.7	46.8	8.5
5	26.3	34.6	17.6	44.8	25.3	5.0
6	22.0	31.1	17.8	42.2	49.7	–
Average E_T (GPa)	23.3	45.7	30.2	42.1	33.0	8.1
Standard deviation (GPa)	3.4	13.0	14.1	1.5	12.4	2.8

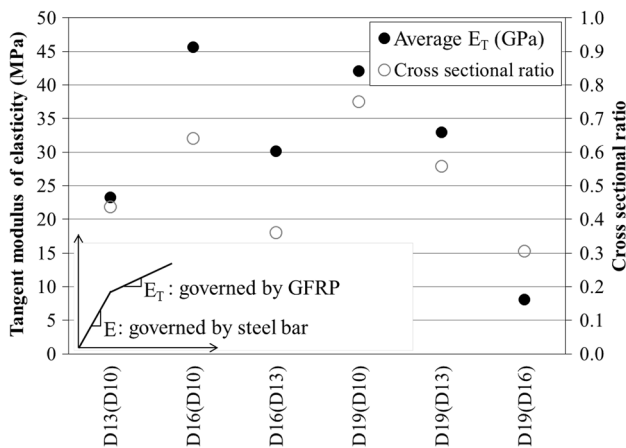


Fig. 10 Relationship between tangent modulus of elasticity and cross sectional ratio.

5. A Suggestion of Stress–Strain Relationship for the GFRP Hybrid Bar

In this study, the tensile property of the GFRP hybrid bar with varying cross sectional ratios was investigated. Among the test specimens, the D19(D10) hybrid bar was found to be the most appropriate hybrid bar in terms of the mechanical properties such as tensile strength and modulus of elasticity. A stress–strain prediction model was suggested on the basis of the experimental tests. The model was derived in a non-linear manner rather than a bi-linear one. The Basic form of the model was adopted from the stress–strain curve of the concrete compressive behavior (Popovics 1970) arising as result of to the similarity and simplicity at the ascending branch until failure. This approach was intended to guarantee the familiarity and practicality in the use of the suggested model. In order to obtain the desired characteristics, model parameters that were significantly different from those of the

stress–strain curve for the concrete compressive behavior were used. One of the changes was the use of a modulus ratio between E and E_T . The tangent modulus of elasticity is one of the important factors determining the tensile property of the GFRP hybrid bar. The E_T could be estimated by following its close correlation with the cross sectional ratio investigated above. The other change was using three kinds of fitting coefficients. These curve fitting factors were finally determined by an iteration process as compared to the experimental results. Therefore, Eq. (1) was introduced for the modified and suggested stress–strain model of the GFRP hybrid bar.

$$f = f_{fu} \times \left(2 \left(\frac{\varepsilon}{\varepsilon_f} \right)^{0.48} - \left(\frac{E_T}{E} \right)^{0.01} \left(\frac{\varepsilon}{\varepsilon_f} \right)^{0.3} \right), \quad (1)$$

where f_{fu} = ultimate stress of the GFRP hybrid bar (MPa), ε = characteristic strain, ε_f = strain according to ultimate stress, E_T = average tangent modulus of elasticity (MPa), E = average modulus of elasticity (MPa)

The conclusive hybrid bar was experimentally selected as D19(D10) hybrid bar in this study and the stress–strain model was proposed for the bar. Figure 11 compares the results of the stress–strain behavior for six experimental results of the D19(D10) hybrid bar and the stress–strain model suggested. The strain at $L/2$ was considered as representative data. The specimens under consideration exhibited the least discrepancy in stress–strain behavior. From the comparison, it was found that the stress–strain behavior of the suggested model was in good agreement with the experimental results. However, the discrepancy slightly increased upon reaching the ultimate stress. The average tensile strength was calculated to be 899.2 MPa, and the standard deviation was found to be 42.0 MPa. For the design value, the design tensile strength of the GFRP exposed to the

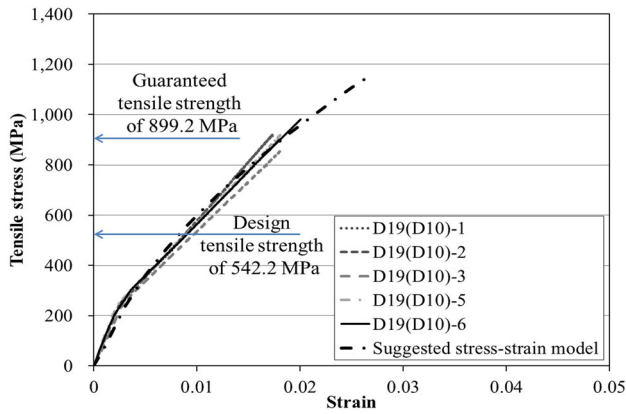


Fig. 11 Tensile stress–strain for suggesting design modulus of elasticity of the GFRP hybrid bar.

surroundings with an environmental factor of 0.7 was determined to be 542.2 MPa. The suggested stress–strain model could accurately predict the tensile behavior including the branch of the tangent modulus of elasticity for the design tensile strength as well as the guaranteed strength.

6. Conclusions

In this study, we developed the GFRP hybrid bar with a core of deformed steel bar to enhance the modulus of elasticity and corrosion resistance. A uniaxial tensile test was carried out and the tensile strength and modulus of elasticity were investigated. A modified stress–strain model was proposed to improve the material properties. Conclusions are as follows:

1. The tensile test revealed that the GFRP hybrid bar showed a low ultimate strength and large modulus of elasticity as compared to the normal GFRP bar. The bi-linear behavior of the GFRP hybrid bar indicated good ductility as compared to the brittle failure of the normal GFRP bar at the ultimate state without any sign of fracture. From the relationship between the tensile strength and modulus of elasticity, it was found that the reasonable criterion for the section design could be determined from the intersection point. D19(D10) specimen showed the largest increase of tensile strength up to 97.8% as compared to that of the yield strength of steel core. The hybridization of the GFRP and steel core could devote to the higher tensile strength than the steel core and the higher modulus of elasticity than the normal GFRP bar.
2. The tangent modulus of elasticity is one of the important factors determining the strength limit state of the GFRP hybrid bar. From the relationship between the tensile strength and the tangent modulus of elasticity, it was found that the D19(D10) bar exhibited an enhanced modulus of elasticity of up to 54.9% as compared to that of the normal GFRP bar and the highest tangent modulus of elasticity among the D19 hybrid bars. Besides, it showed the most stable behavior in tensile

test. Therefore, the cross sectional design of the D19(D10) hybrid bar was considered to be most appropriate. Bars with this cross sectional design can be used as reinforcements to design, analyze, and construct concrete bridge deck slabs.

3. The conclusive hybrid bar was experimentally selected as D19(D10) hybrid bar in this study and the stress–strain model was proposed for the bar. The proposed model showed a good agreement with the experimental tests. The stress–strain model could accurately predict the tensile behavior including the branch of the tangent modulus of elasticity for the design tensile strength and strength. This stress–strain model can be applied to structural designs or finite element analysis for flexural RCs or concrete bridge deck slabs. Further investigation on various bar diameters and flexural performance needs to be carried out including the effect of the GFRP outer surface only to the tensile characteristics of the GFRP hybrid bars.

Acknowledgements

This research was supported by a Construction Technology Research Project (17SCIP-B128706-01) funded by the Ministry of Land, Infrastructure and Transport and Basic Science Research Program through the National Research Foundation of Korea (NRF) funded by the Ministry of Education (NRF-2016R1D1A1B03934809).

Open Access

This article is distributed under the terms of the Creative Commons Attribution 4.0 International License (<http://creativecommons.org/licenses/by/4.0/>), which permits unrestricted use, distribution, and reproduction in any medium, provided you give appropriate credit to the original author(s) and the source, provide a link to the Creative Commons license, and indicate if changes were made.

References

- AASHTO. LRFD. (2009). *Bridge design guide specifications for GFRP-Reinforced concrete bridge decks and traffic railings*. Washington, DC, USA: American Association of State Highway and Transportation Officials.
- ACI Committee 440. (2004). *Guide test methods for fiber-reinforced polymers (FRPs) for reinforcing or strengthening concrete structures (ACI 440.3R-04)*. Farmington Hills, MI, USA: American Concrete Institute.
- ACI Committee 440. (2015). *Guide for the design and construction of concrete reinforced with FRP bars (ACI 440.1R-15)*. Farmington Hills, MI, USA: American Concrete Institute.

- ASTM D 3916. (2002). *Standard test method for tensile properties of pultruded glass fiber reinforced plastic rods*. West Conshohocken, PA: American Standard Test Method
- CAN/CSA S806-12. (2012). *Design and construction of building structures with fibre-reinforced polymers*. Ontario, Canada: Canadian Standards Association/National Standard of Canada.
- Carvelli, V., Pisani, M. A., & Poggi, C. (2010). Fatigue behavior of concrete bridge deck slabs reinforced with GFRP bars. *Composites Part B, 41*(7), 560–567.
- Choi, O. C., Jung, S. Y., & Park, Y. S. (2006). Corrosion evaluation of epoxy-coated bars in chloride contaminated concrete using linear polarization tests. *International Journal of Concrete Structures and Materials, 18*(1E), 03–09.
- Choi, O. C., Park, Y. S., & Ryu, H. Y. (2008). Corrosion evaluation of epoxy-coated bars by electrochemical impedance spectroscopy. *International Journal of Concrete Structures and Materials, 2*(2), 99–105.
- El-Gamal, S. E., El-Salakawy, E. F., & Benmokrane, B. (2007). Influence of reinforcement on the behavior of concrete bridge deck slabs reinforced with FRP bars. *ASCE, Journal of Composites for Construction, 11*(5), 449–458.
- El-Gamal, S. E., El-Salakawy, E. F., & Benmokrane, B. (2009). Durability and structural performance of carbon fibre reinforced polymer-reinforced concrete parking garage slabs. *Canadian Journal of Civil Engineering, 36*(4), 617–627.
- El-Refai, A., Abed, F., & Al-Rahmani, A. (2015). Structural performance and serviceability of concrete beams reinforced with hybrid (GFRP and steel) bars. *Construction and Building Materials, 96*, 518–529.
- Lau, D., & Pam, H. J. (2010). Experimental study of hybrid FRP reinforced concrete beams. *Engineering Structures, 32*(12), 3857–3865.
- Maranan, G. B., Manalo, A. C., Benmokrane, B., Karunasena, W., & Mendis, P. (2015). Evaluation of the flexural strength and serviceability of geopolymer concrete beams reinforced with glass-fibre-reinforced polymer (GFRP) bars. *Engineering Structures, 100*, 529–541.
- Mazaheripour, H., Barros, J. A. O., Soltanzadeh, F., & Sena-Cruz, J. (2016). Deflection and cracking behavior of SFRSCC beams reinforced with hybrid prestressed GFRP and steel reinforcements. *Engineering Structures, 125*, 546–565.
- Nanni, A., Henneke, M. J., & Okamoto, T. (1994). Tensile properties of hybrid rods for concrete reinforcement. *Construction and Building Materials, 8*(1), 27–34.
- Park, C., Park, Y., Kim, S., & Ju, M. (2016). New emerging surface treatment of hybrid GFRP bar for stronger durability of concrete structures. *Smart Structures and Systems, 17*(4), 593–610.
- Popovics, S. A. (1970). Review of stress-strain relationships for concrete. *ACI Structural Journal, 67*(3), 243–248.
- Pritzl, M. D., Tabatabai, H., & Ghorbanpoor, A. (2014). Laboratory evaluation of select methods of corrosion prevention in reinforced concrete bridges. *International Journal of Concrete Structures and Materials, 8*(3), 201–212.
- Seo, D. W., Park, K. T., You, Y. J., & Kim, H. Y. (2013). Enhancement in elastic modulus of GFRP bars by material hybridization. *Scientific Research, 5*, 865–869.
- Tae, S. H. (2006). Corrosion resistance of Cr-bearing rebar to macrocell corrosion environment induced by localized carbonation. *International Journal of Concrete Structures and Materials, 18*(1E), 17–22.
- You, Y. J., Park, Y. H., Kim, H. Y., & Park, J. S. (2007). Hybrid effect on tensile properties of FRP rods with various material composition. *Composite Structures, 80*, 117–122.
- You, Y. J., Kim, J. H., Park, Y. H., & Choi, J. H. (2015). Fatigue performance of bridge deck reinforced with cost-to-performance optimized GFRP rebar with 900 MPa guaranteed tensile strength. *Journal of Advanced Concrete Technology, 13*, 252–262.
- Zheng, Y., Li, C., & Yu, G. (2012). Investigation of structural behaviors of laterally restrained GFRP reinforced concrete slabs. *Composites Part B, 43*(3), 1586–1597.